NIH Public Access
Author Manuscript

Characterization of the Gene Expression Profile of Human *Bocavirus*

Aaron Yun Chen[1,#], **Fang Cheng**[1,#], **Sai Lou**[1,2], **Yong Luo**[1], **Zhengwen Liu**[2], **Eric Delwart**[3], **David Pintel**[4], and **Jianming Qiu**[1,*]

[1] Department of Microbiology, Molecular Genetics and Immunology University of Kansas Medical Center, Kansas City, Kansas

[2] Department of Infectious Diseases, The First Affiliated Hospital Xi'an Jiaotong University, Xi'an, China

[3] Blood Systems Research Institute, San Francisco, California

[4] Life Sciences Center, University of Missouri-Columbia, Columbia, Missouri

Abstract

We have generated a quantitative transcription profile of human bocavirus type 1 (HBoV1) by transfecting a nearly full-length clone in human lung epithelial A549 cells as well as in a replication competent system in 293 cells. The overall transcription profile of HBoV1 is similar to that of two other members of genus *Bocavirus*, minute virus of canines and bovine parvovirus 1. In particular, a spliced NS1-transcript that was not recognized previously expressed the large non-structural protein NS1 at approximately 100 kDa; and the NP1-encoding transcripts were expressed abundantly. In addition, the protein expression profile of human bocavirus type 2 (HBoV2) was examined in parallel by transfection of a nearly full-length clone in A549 cells, which is similar to that of HBoV1. Moreover, our results showed that, unlike human parvovirus B19 infection, expression of the HBoV1 proteins only does not induce cell cycle arrest and apoptosis of A549 cells.

Introduction

Human *Bocavirus* (HBoV) is one of the recently identified respiratory viruses, and tentatively is classified in the genus *Bocavirus* within the subfamily of *Parvovirinae* of the *Parvoviridae* family (Cotmore and Tattersall, 2005). Other members in the *Bocavirus* genus are bovine parvovirus type 1 (BPV1) (Chen et al., 1986), minute virus of canines (MVC) (Schwartz et al., 2002). Different species of HBoV have been identified in humans including the prototype HBoV in respiratory samples as well as HBoV2 and HBoV3 in feces (Kapoor et al., 2009; Arthur et al., 2009).

HBoV1 was initially identified from nasopharyngeal aspirates of patients with lower respiratory infections (Allander et al., 2005). The HBoV1 genome has been frequently detected worldwide, ranging from 2%–19% in respiratory specimens from children under two years old

with acute respiratory illnesses (Allander et al., 2005; Arden et al., 2006; Arnold et al., 2006; Bastien et al., 2006; Choi et al., 2006; Foulongne et al., 2006; Ma et al., 2006; Sloots et al., 2006; Weissbrich et al., 2006; Lin et al., 2008; Lin et al., 2007). HBoV1 is associated with acute expiratory wheezing and pneumonia (Allander et al., 2007; Kahn, 2008; Schildgen et al., 2008), and is commonly detected in association with other respiratory viruses (Kahn, 2008; Schildgen et al., 2008). However, HBoV1 acute infection with high viral loads in respiratory samples (>10,000 copies/ml) and increased IgG or IgM detection have been frequently associated with acute respiratory illnesses (Allander et al., 2005; Kantola et al., 2008), which indicates an apparent etiological link to respiratory illnesses. In addition to respiratory illnesses, HBoV1 is associated with gastroenteritic diseases (Lee et al., 2007; Arnold et al., 2006; Lau et al., 2007; Vicente et al., 2007; Albuquerque et al., 2007), a characteristic that shares with two closely related animal bocaviruses. The largest genome of HBoV1 that has been sequenced is 5,299 nts, which lacks both termini; therefore, it is not infectious. To date, both termini of the HBoV genome have not been sequenced; therefore, an HBoV1 infectious DNA clone has not been described. Recently, new species of human *Bocavirus*, HBoV2 and HBoV3, were identified in human stool specimens. HBoV2 has a genomic organization identical to that of HBoV1, but the HBoV2 NS1, NP1, and VP1 proteins have only 78%, 67%, and 80% identity to those of HBoV1, respectively. Further studies are necessary, however, to identify potential associations of HBoV2 and HBoV3 with clinical symptoms or disease (Kapoor et al., 2009; Arthur et al., 2009).

A cell culture system of HBoV1 infection has been recently established (Dijkman et al., 2009); however, it is inefficient in that HBoV1 transcripts were only detected by reverse-transcription (RT)-PCR. Six transcripts of HBoV1 were identified from HBoV1-infected differentiated human airway epithelial cells (Dijkman et al., 2009). The abundance of these transcripts and their coding capabilities are not yet understood. Two non-structural proteins NS1 and NP1 were predicted, but the NS1 seems to lack the C-terminus compared to the full length NS1 of BPV1 and MVC (Qiu et al., 2007; Sun et al., 2009). The full length sequence of infectious MVC DNA (Genbank accession no.: FJ214110) shows 52.6% identity to HBoV1, while the NS1, NP1 and VP1 proteins of MVC are 38.5%, 39.9% and 43.7% identical to those of HBoV1, respectively (Sun et al., 2009). We have previously determined the transcription profiles of the BPV1 and MVC during infection (Qiu et al., 2007; Sun et al., 2009). In BPV1, the left ORF encodes the non-structural protein NS1, at approximately 100 kDa, and proteins at relatively small sizes are proposed as NS2 (Qiu et al., 2007; Lederman et al., 1987). The mid-ORF is thought to encode the BPV1 abundant non-structural protein NP1 at 28 kDa, and the right ORF contains the coding sequences for the overlapping capsid protein genes VP1 and VP2 (Qiu et al., 2007; Lederman et al., 1987). Both the NS1 and NP1 of MVC are important in DNA replication of MVC (Sun et al., 2009). The NP1 of HBoV1 and BPV1 can supplement the lack of function of the MVC NP1 in replication of an NP1 knock-out MVC infectious clone to some degree (Sun et al., 2009); however, the NP1 proteins of the bocaviruses share no similarity to any proteins of the other parvoviruses. Detection of HBoV proteins either during infection or in transfection has not been reported.

In this study, we generated a comprehensive transcription profile of HBoV1 by transfecting a replicative chimeric HBoV1 genome in 293 cells and a non-replicative genome in A549 cells. We studied the expression profiles of both the structural and non-structural proteins of HBoV in detail. Transcripts encoding the left ORF (NS1) are either spliced or unspliced at a small intron that lies in the middle of the genome. Thus, the spliced transcripts are able to encode a large nonstructural protein NS1 at approximately 100 kDa, which is comparable to the NS1 of MVC and BPV1; while the unspliced transcripts encode a relatively small nonstructural protein NS1-70 at approximately 70 kDa.

Results

Determine the relative abundance of HBoV1 transcripts by RNase protection assay (RPA)

A transcription map of the HBoV1 has been reported, which was obtained from HBoV1 RNA isolated from HBoV1-infected differentiated human airway epithelial cells (Dijkman et al., 2009). In that report, the HBoV1 transcripts were identified by reverse transcription (RT)-PCR; therefore, the relative abundance of the individual transcripts could not be determined. In other parvovirus systems, little difference has been seen between viral infection and plasmid transfection (Qiu et al., 2002; Qiu et al., 2005; Qiu et al., 2007; Sun et al., 2009). Therefore, we decided to examine the HBoV1 transcription profile in detail by transfection. To this end, we constructed an HBoV1 plasmid (pHBoV1) containing the full HBoV1 coding sequence (nt 1- 5299) by amplifying a nearly full-length genome from an HBoV1-positive nasopharyngeal aspirate sample. The sequence of this clone was deposited in Genbank (access no.: GQ925675). We have found previously that the status of replication alters the transcription profile of human parvovirus B19 (B19V) (Guan et al., 2008). To observe the transcriptional profile in a replication-competent system, we inserted the HBoV1 genome into adeno-associated virus type 5 (AAV5) inverted terminal repeats (ITRs) so that it could be replicated while AAV5 Rep78 and necessary Ad5 genes were provided (Guan et al., 2008) in 293 cells (data not shown).

We used mRNAs isolated from two sources for transcript mapping: those from A549 cells transfected with pHBoV1, and those from 293 cells transfected with p5TRHBoV1/pHIVAV5Rep78/phelper. RT-PCR and 5′/3′ RACE were performed as previously described (Qiu et al., 2002; Qiu et al., 2005; Qiu et al., 2007; Sun et al., 2009), and gel purified PCR fragments were further sequenced (data not shown). The RNA landmarks determined by transfection of p5TRHBoV1 in 293 cells, which were the same as those determined by transfection of pHBoV1 in A549 cells, are depicted and diagramed to scale in Fig. 1A. These landmarks basically confirmed the transcription units as identified in the previously reported virus infection system (Dijkman et al., 2009), with the exception of an extra splice site (A1-1) in the first intron. This A1-1 splice site is present in BPV1 RNA during BPV1 infection (Qiu et al., 2007), but not in MVC RNA from MVC infection (Sun et al., 2009).

To determine the relative abundance of each HBoV1 mRNA, we used 7 anti-sense HBoV1 probes to protect individual HBoV1 mRNA. A schematic diagram of the 7 anti-sense HBoV1 probes with their putative protected bands and nucleotide numbers (nt) is shown in Fig. 1A.

Probe PD1—Probe PD1, spanning the putative promoter (P3) and the first donor site (D1), protected bands of 133 and 55 nts. These bands mapped the RNA initiation site at nt 187 and the first splice donor site (D1) at nt 242. Similar to that of BPV1 and MVC, the first exon of HBoV is short, containing only 55 nts (Fig. 1B, lane 2). Approximately 75% of HBoV1 RNAs were spliced at the D1 donor site. Multiple bands centralized at nt 55 were considered as spliced RNA (Qiu et al., 2002).

Probe PA1-1—Probe PA1-1, spanning the first acceptor site of the first intron (A1-1), protected bands of 182 and 120 nts (Fig. 1B, lane 3). The 120-nt band mapped the first 3′ splice acceptor site at nt 920, which is similar to the location of the acceptor site in BPV1 RNA. In addition, as seen in BPV1, only a small portion of RNAs, less than 10% of spliced RNA at the D1 donor site, were spliced at the A1-1 acceptor site (Qiu et al., 2007).

Probe PA1-2 and PA1-2/D2—Probe PA1-2, spanning the second acceptor of the first intron (A1-2), protected bands of 162 and 117 nts (Fig. 1C, lane 2). Probe PA1-2/D2, spanning the second acceptor of the first intron (A1-2) and the donor site of the small intron (D2), protected bands of 225, 122 and 168 nts (Fig. 1C, lane 3). These bands protected from both probes confirmed the location of the A1-2 acceptor and the D2 donor at nt 2043 and nt 2165,

respectively. Similar to BPV1 and MVC, the majority of HBoV1 RNAs protected by probe PA1-2/D2 were spliced at both sites, resulting in the abundant band present at 122 nts (approximately 90%). Only approximately 5% of RNAs in this region were unspliced at the A1-2 acceptor site, which resulted in the band at 168 nts (spliced at D2) and the band at 225 nts (unspliced at D2). Interestingly, this probe did not detect RNAs that were spliced at A1-2 and remained unspliced at the D2 site (which would have generated a band at 181 nts).

Probe A2/D3—Probe PA2/D3, which spans the A2 acceptor and the D3 donor sites, protected bands at 241, 123, 192 and 167 nts. These bands confirmed the usage of the A2 site at nt 2235 and the D3 site at nt 2358 (Fig. 1D, lane 2). Approximately an half of the RNAs that spliced the small intron (D2-A2) were not further spliced at the third intron (D3-A3), which resulted in the 192-nt band; another half were spliced at D3, which resulted in the 123-nt band. These spliced mRNAs at 123 nts (spliced at both A2 and D3, Fig. 1D, lane 2) represent capsid protein-encoding mRNAs, which account for one third of the RNAs protected by probe A2/D3. Only a minor portion of RNAs, at a size of 167 nts, were unspliced at the A2 site and spliced at the D3 site (Fig. 1D, lane 2), which was not seen in RNAs from transfected A549 cells (data not shown); therefore, we did not include this transcript in the final transcription profile.

Probe PA3—Probe PA3, which spans the A3 acceptor site, protected two bands at 159 and 107 nts. Thus the A3 acceptor site was mapped to nt 2995 (Fig. 1E, lane 2). The ratio of unspliced to spliced RNA across this region was approximately 1:1.

Probe P(pA)p—Probe P(pA)p was used to map the internal poly A signal (pA)p (Fig. 1E, lane 3). The band at 108 nts mapped the cleavage site at 3406, consistent with the site identified by 3′RACE (data not shown). The ratio of RNAs that read-through *vs.* those polyadenylated at (pA)p was approximately 1:1. The AAUAAA at nt 3232 was not used (data not shown).

Northern blot analysis of HBoV1 RNA

From the results obtained from RT-PCR and RPA, we obtained a preliminary transcription map of HBoV1 expression by transfection (Fig. 2B). We next sought to determine the abundance of these HBoV1 transcripts by Northern blot analysis using three probes that are schematically diagramed at the bottom of Fig. 2B.

Hybridization of HBoV1 RNAs, either from 293 cells (replication-competent) or A549 cells, with the *Cap* probe revealed HBoV1 transcripts that were polyadenylated at the (pA)d site (Fig. 2A, lanes 2&3). These transcripts were the 4.8 kb R2M mRNA and the 4.9 kb R2m mRNA, which putatively encode NS1, the 3.0 kb R4 mRNA - putatively encoding NP1 as well as the 2.4 kb R5 mRNA - putatively encoding capsid protein VP1 and VP2. The R6 mRNA that was detected in HBoV1 RNA from infected cells (Dijkman et al., 2009) was predicted to hybridize with the *Cap* probe at a size of 2.3 kb. The R7 mRNA, which is similar to that encoding MVC and BPV1 capsid proteins, was detected by RT-PCR in RNAs isolated from both transfection systems (data not shown); it was predicted to hybridize with the *Cap* probe at a size of 2.1 kb (Fig. 2A, lanes 2&3). Since the Northern blot did not resolve the bands at sizes of 2.1, 2.2 and 2.4 kb very well, we assume that all the R5, R6 and R7 are putative mRNAs to encode capsid proteins (Fig. 3A).

The *NS* probe should detect all the species of HBoV1 RNAs because they are generated from a single promoter and share the same first exon (only 60 nts). Similar to MVC and BPV1 RNAs, the first exon is short, and the *NS* probe hybridized to these first-exon-containing RNAs poorly; therefore, hybridization of HBoV1 RNAs with the *NS* probe only revealed two abundant RNA species, i.e. R1M at 3.1 kb and R2M at 4.8 kb (Fig. 2, lanes 4&5), both of which could encode NS1. R1m RNA at 3.2 kb was not clearly detected in either HBoV1 RNA sample.

Northern analysis with the whole HBoV1 genomic probe (*NSCap*) revealed the overall HBoV1-generated RNA profiles from transfection of both replicative and non-replicative plasmids (Fig. 2A, lanes 6&7, respectively). Eight major species of RNAs were detected, and these were consistent in size with RNAs predicted to encode NS1 (R1M and R2M mRNA at 3.1 and 4.8 kb, respectively), NS1-70 (R2m mRNA at 4.9 kb), NP1 (R3 and R4 mRNAs at 1.3 and 3.0 kb, respectively), and VP1/2 (R5, R6 and R7 mRNA at 2.4, 2.2 and 2.1 kb, respectively). R3 and R4 mRNAs, both of which could encode NP1, are the most abundant RNAs and account for approximately 50% of total HBoV1 RNAs (Fig. 2A, lanes 6&7, 1.3 and 3.0 kb). The overall abundance of the R5, R6 and R7 capsid protein-encoding mRNAs constitute approximately one third of total HBoV1 RNAs (Fig. 3A).

Although the A1-1 acceptor was shown by the RPA using a probe spanning the acceptor, the R8 and R9 mRNAs, which may use alternative polyadenylation, were not clearly hybridized as bands at 1.8 kb and 3.5 kb. Similar mRNAs were obvious on the Northern-blot of BPV-1 RNA but not on the blot with MVC RNA (Sun et al., 2009). Interestingly, in HBoV1 RNAs extracted from infected cells, such spliced R8 and R9 mRNAs were not detected by RT-PCR (Dijkman et al., 2009). However, since tissue-specific splicing has been observed in parvovirus MVM pre-mRNA processing (Choi et al., 2005), the significance of the R8 and R9 mRNAs awaits further investigation. A band at approximately 1.8 kb, indicated by an asterisk in Fig. 2A, was always detected by all the three probes but not in RNAs extracted from mock transfected cells (data not show). The nature of this 1.8 kb band is currently unknown; however, a similar band was also detected in Northern blot analysis of MVC RNA (Sun et al., 2009).

Summarizing results from RPA and Northern blot analysis, we generated a genetic map of HBoV1, which is shown in Fig. 3A. Eight major species of HBoV1 mRNAs are shown with their respective sizes, abundance in percentage and proteins to encode. This revised map is very similar to that of MVC (Sun et al., 2009).

Expression of HBoV proteins

Next, we used the transcription map as a guide to profile HBoV1 non-structural proteins expressed by transfection. First, we tagged an HA-tag to the N-terminus of the NS1 ORF in the full length clone of pHBoV1 to make HA-NS1-expressing plasmid pHBoV1(HA-NS1), and an HA-tag to the C-terminus of the NP1 ORF in pHBoV1 to make NP1-HA-expressing plasmid pHBoV1(NP1-HA). Transfection of pHBoV1(HA-NS1) revealed two bands at approximately 100 kDa and 70 kDa (Fig. 4A), confirming that R1M and R2M mRNAs encode the large NS1 protein, and R2m mRNA encodes the small NS1-70 protein. Transfecting pHBoV1(NP1-HA) confirmed the expression of NP1 at approximately 26 kDa from R3 and R4 mRNA (Fig. 4A, lane 3).

Since a large size of the NS1 (at ~100k Da) was detected in cells transfected with pHBoV1, we aligned the C-terminus of the NS1 proteins of HBoV1, BPV and MVC, as shown in Fig. 3B, using ClustalW2 (Larkin et al., 2007). The result showed that there are two conserved motifs, 740WGERLGLI747 and 757PIVLXCFE764, present at the C-terminus of the *Bocavirus* (Fig. 3B). We were not able to identify similar motifs in the NCBI BLAST database (http://www.ncbi.nlm.nih.gov/Structure/cdd/wrpsb.cgi), suggesting that they are highly conserved motifs among members of the genus *Bocavirus*. However, the search engine failed to identify any known domain with expected value lower than 1. Nevertheless, the potential role of these highly conserved motifs of *Bocavirus* NS1 C-terminus warrants further study.

To further confirm results obtained from the two HA-tagged constructs and the conserved C-terminus of the NS1, we raised antiserum against the C-terminus of NS1, which shares a portion of coding sequences with NP1 but in different frames, and antiserum against the whole NP1, respectively. Western blot analysis of cell lysate from pHBoV1-transfected cells with anti-NS1

(C-terminus) antiserum revealed three major bands, at approximately 100, 66 and 34 kDa, respectively (Fig. 4B, lane 2). The sizes of these bands were confirmed by resolving the NS1 proteins on SDS-6% and -12% PAGE gels, respectively (Fig. 4B).

This antiserum did not react with the NS1-70 (Fig. 4B, lane 1). Thus we have determined that the HBoV1 NS1 was expressed as a full length protein of 100 kDa, and small proteins at 66 kDa and 34 kDa, respectively. The mechanism by which the C-terminal 66-kDa (NS1*66) and 34-kDa (NS1*34) proteins were generated is currently unknown. Interestingly, similar small NS1 proteins were detected in pHBoV2-transfected cells (Fig. 4B, lane 3). The intact HBoV1 and HBoV2 NS1 were detected at approximately 100 kDa rather than at the putative size at 85 kDa (Sun et al., 2009), indicating a modification, perhaps phosphorylation, of both NS1. The sizes of HBoV2 NS1 and NS1*66 were further confirmed by resolving the NS1 proteins on an SDS-6%PAGE gel (Fig. 4B, 6%PAGE, lane 2). As expected, the anti-HBoV1 NP1 antiserum detected both HBoV1 and HBoV2 NP1 at approximately 26 kDa in transfected cells (Fig. 4C, lanes 1&2), suggesting they are not modified unlike the HBoV1&2 NS1 proteins.

We chose GST-fused HBoV1 VP1 peptide of aa 369–475 to generate antiserum. In this region, two identical domains, aa 380–400/aa376–396 and aa 422–440/aa418–436, are present both in HBoV1 and HBoV2 VP1. By using the anti-VP1 antiserum, we confirmed the putative VP1 and VP2 of both HBoV1 and HBoV2 at approximately 72 and 60 kDa, respectively (Fig. 4D). The anti-VP1/2 antiserum cross reacted with a cellular protein at a size of approximately 90 kDa as indicated by an arrow (Fig. 4D). These results suggest a similar expression of NS1, NP1 and VP1/2 between the two species of HBoV. Moreover, the conserved expression of the small NS1*66 in cells transfected with both pHBoV1 and pHBoV2 suggest that it must be important in *Bocavirus* infection.

Proteins at sizes of 47 kDa, potentially expressed from putative R8 and R9 mRNAs, were not detected with anti-HA, anti-NS1 or anti-NP1 antiserum, further supporting that mRNA spliced at A1-1 may not be significant. In addition, protein bands at 17.5 and 8.8 kDa, which include putative UP1 and UP2 ORFs, respectively, from the previously identified map of HBoV1 generated from HBoV1-infected cells (Fig. 2B) (Dijkman et al., 2009), were not detected in pHBoV1&2-transfected cells by either anti-NS1 (Fig. 4B, lanes 2&3) or anti-HA (Fig. 4A, lanes 2&3).

A genetic map of HBoV1 summarizing the results of the experiments so far described is shown in Fig. 3A. Collectively, R1M and R2M mRNAs encode the large NS1 protein at a size of approximately 100 kDa. The HBoV1 NS1 protein apparently was modified, perhaps phosphorylated, since its coding capability is only 86 kDa. Interestingly, at least two small stable NS1 proteins, NS1*66 and NS1*34 at 66 and 34 kDa, respectively, were expressed by transfection in A549 cells, which share the C-terminus with that of the full length NS1.

Cellular localization of HBoV proteins

We next examined the cellular localization of HBoV1 proteins by transfection of pHBoV1 in A549 cells. Staining with ant-NS1 C-terminus antiserum showed a clear nuclear staining (Fig. 5, NS1), suggesting that the NS1, NS1*66 and NS1*34 were localized in the nucleus. Furthermore, anti-NP1 staining showed that the NP1 was localized in the nucleus as well (Fig. 5, NP1). These results suggest that the NS1 and NP1 of the HBoV1 have their potential function in HBoV DNA replication, similar to those of MVC (Sun et al., 2009; Chen et al., 10 A.D.). The HBoV1 VP1 and VP2, as stained with anti-VP1/2 antiserum, were basically localized in the nucleus with some diffused cytoplasmic staining (Fig. 5, VP1/2), similar to the capsid proteins of other parvoviruses (Vihinen-Ranta and Parish, 2006).

Expression of all HBoV1 proteins does not induce apoptosis or cell cycle arrest

The large non-structural protein NS1 of other parvoviruses, e.g. the NS1 of MVM, H-1 and B19V, has been shown to induce apoptosis and/or cell cycle arrest of transfected cells (Brandenburger et al., 1990; Daeffler et al., 2003; Ozawa et al., 1988; Rayet et al., 1998; Sol et al., 1999). The cytopathic and cell cycle regulatory effect elicited during viral infection is important in the virus life cycle, particularly for viral DNA replication and virus egress. Therefore, we decided to examine the apoptotic cell death and cell cycle regulation induced by HBoV1 viral proteins. We transfected the HBoV1 non-replicative construct pHBoV1 into A549 cells. Transfected cells were analyzed for cell cycle and apoptosis by DAPI and FLICA staining, respectively. Both NS1-expessing and non-expressing cell populations were gated and plotted for comparison (Fig. 6). Expression of the NS1, NS1*66, NS1*34, NS1-70, NP1 and VP1/VP2 of HBoV1 in transfected cells were detected by Western-blot (Fig. 4). However, transfection of pHBoV1 did not induce an obvious cell cycle change and apoptotic cell death in NS1 expressing cells (NS+) compared to those in NS1(−) cell population [Fig. 6, compare numbers in NS+ with NS1(−)]. Active caspase is a hallmark of apoptotic cell death (Degterev et al., 2003). Thus, our results suggest that expression of both HBoV1 non-structural and structural proteins does not induce an apparent apoptosis or a perturbation of cell cycle progression in transfected cells.

Discussion

HBoV RNA profile

In this paper, we report a detailed characterization of the expression profile of *Bocavirus* HBoV1. The HBoV1 profile was obtained from RNAs following transfections. Analysis of HBoV1 RNA produced during infection quantitatively by Northern or RNase protection assay is currently precluded by the lack of isolated viruses at a high load and the low efficiency of virus replication (Dijkman et al., 2009). However, previous analysis of RNAs generated by plasmid transfection of simian parvovirus (Liu et al., 2004), B19V (Guan et al., 2008) and adeno-associated viruses (Qiu and Pintel, 2002; Qiu et al., 2002) show similar profiles to those seen in virus infections. Our results showed that the overall transcription profile of HBoV1 is similar to that of two other *Bocavirus* members, MVC and BPV1 (Sun et al., 2009; Qiu et al., 2007), in that all the species of HBoV1 mRNAs are transcribed from a single promoter and further processed through alternative splicing and alternative polyadenylation. These features are also similar to the transcription profiles of members in the genera *Erythrovirus* and *Amdovirus* (Ozawa et al., 1987; Liu et al., 2004; Qiu et al., 2006), which highlights the importance of the regulation of alternative polyadenylation in the expression of parvovirus genomes that have a single promoter (Qiu and Pintel, 2008).

HBoV protein expression

We observed two major species of HBoV1 mRNAs, the spliced R1M and R2M mRNAs, in HBoV1 RNA from transfected cells. These mRNA species were not recognized previously (Dijkman et al., 2009). The R1M and R2M mRNAs were spliced at the small intron at a level of approximately 60% (Fig. 1C). In addition, a corresponding protein NS1, which contains a C-terminus of aa 639–781, was detected in HBoV1 transfected cells. This result suggests that the NS1 must be encoded by the R1M and R2M mRNAs, through which the NS1 ORF extends its C-terminus by removing the small intron (Fig. 3). The encoding sequence of the extended NS1 C-terminus overlaps with the NP1-encoding sequence, but in different frames. Moreover, both MVC and BPV1 encode an NS1, which has the C-terminus-encoding sequences overlapped with the NP1-encoding sequence (Qiu et al., 2007; Sun et al., 2009). BPV1 NS1 protein is expressed at a size of approximately 100 kDa (Qiu et al., 2007). The large nonstructural protein NS1 of parvovirus is a multifunctional protein that plays a key role in virus replication. It possesses a site-specific DNA binding domain at the N-terminus, a

transcription activation domain at the C-terminus, and enzymatic domains of ATPase and helicase in the middle (Cotmore and Tattersall, 2006). The C-terminus of HBoV1 NS1 does not share any similarities with that of the NS1 of other parvoviruses except for the NS1 of MVC and BPV1. The NS1 C-terminus of the three *Bocavirus* members shares 50% of consensus sequences and 27% identity, especially the two conserved motifs, at the last 44 amino acids (Fig. 3B). Therefore, we believe that the HBoV1 NS1 protein is most likely a typical *Bocavirus* NS1 protein that must have functions, such as transactivation, in virus replication.

Two other non-structural proteins are expressed by HBoV1, NS1-70 and NP1. NS1-70 is likely expressed from unspliced R2m mRNA. The mid-ORF encoded NP1 was expressed at a high level following transfection in comparison with NS1 (Fig. 4A), which is consistent with the abundant level of R3 and R4 mRNAs (Fig. 3A). Unique to all bocaviruses so far characterized is the expression of the mid-ORF-encoded NP1. To our surprise, the NS1 of HBoV1 and HBoV2 are expressed in different sizes, resulting in multiple bands on Western blot analysis (Fig. 4B). Multiple bands centering at 45 kDa also were observed in BPV1 infected cell lysates immunoprecipitated using convalescent sera from BPV1-infected calves (Lederman et al., 1983). Cleavage of AMDV NS1 has been proved to be essential and functional for viral DNA replication (Best et al., 2003). The small bands centralized at 66 kDa were present in both HBoV1&2 NS1 expression, suggesting that this small NS1*66 protein must play a role during virus infection, which is currently under investigation. These multiple small proteins of NS1 might be translated from alternative initiation sites or specifically cleaved by protease. The exact mechanism by which these small NS1 proteins are produced awaits further investigation.

Effect of HBoV proteins on cells

In parvoviruses, the large nonstructural proteins, NS1 (Nuesch and Rommelaere, 2006; Rayet et al., 1998; Sol et al., 1999) or Rep 78 (Schmidt et al., 2000) are pro-apoptotic proteins. Recently, we have identified the small nonstructural protein 11kDa of B19V behaves as a potent apoptosis-inducer during infection (Chen et al., 2010). Parvovirus infection-induced cell death often connects to the pathogeneses of parvovirus infection, e.g., B19V infection-induced cell death of erythroid progenitor cells of bone marrow causes chronic anemia in immunocompromised patients (Young and Brown, 2004). We have recently identified capsid protein expression of AMDV activates caspases (Cheng et al., 2009). Conversely, all the HBoV1 proteins, NS1, NS*66, NS*34, NS1-70, NP1 and VP1/VP2, do not induce apoptosis by transfection (Fig. 6), which is similar to those proteins of MVC, another member in genus *Bocavirus* (Chen et al., 10 A.D.), and maybe a common feature of the *Bocavirus*. We have recently identified that replication of the MVC genome activates caspases that accounts for MVC infection-induced apoptosis (Chen et al., 10 A.D.). However, currently an efficient HBoV infection system has not been established; whether HBoV1 or HBoV2 infection causes cell death and the role of these proteins in the pathogenesis of HBoV infection await further investigation.

Materials and Methods

Cells and transfection

Human alveolar epithelial A549 cells (ATCC CCL-185), human embryonic kidney 293 cells (ATCC CRL-10852) were maintained in Dulbecco's modified Eagle's medium with 10% fetal calf serum in 5% CO_2 at 37°C.

Transfection was performed using the Lipofetamine™ and Plus™ reagent (Invitrogen) or LipoD293 transfection reagent (SignaGen Laboratories) following the manufacturers' instructions.

Plasmid constructs

(i) HBoV constructs—Incomplete HBoV1 and HBoV2 genomes of 5,299 nts were amplified from DNA samples extracted from nasopharyngeal aspirate and stool samples, respectively, with primers based on the published HBoV1 sequence (Genbank accession no.: DQ000496) and HBoV2 sequence (Genbank accession no.: GQ200737)**,** respectively. The HBoV1 and HBoV2 DNAs (nt 1-5299) were cloned into XhoI/XbaI-digested pBluescript SK (+) vector (Strategene), separately, which resulted in pHBoV1 and pHBoV2, respectively. p5TRHBoV1 was made by inserting the HBoV1 sequence (nt 1-5299) into an AAV5 ITRs-containing plasmid, pAV5ITR (Guan et al., 2008); thus, in p5TRHBoV1, the HBoV1 sequence was flanked with AAV5 ITRs at two ends. pHBoV1(HA-NS1) and pHBoV1(NP1-HA) were constructed by inserting an HA tag into nt 259 at the N-terminus of the NS1 ORF and nt 3056 at the C-terminus of the NP1 ORF in pHBoV1, respectively. pHBoV1(NS1-70-HA) was constructed by inserting the NS1-70 ORF of HBoV1 (nt 253-2169) into BamHI/XhoI-digested pcDNA3CHA. The pcDNA3CHA vector was constructed by inserting three repeated HA tag between XhoI and XbaI sites into pcDNA3 (Stratagene).

(ii) Constructs for RNA probe generation—HBoV1 transcription units were mapped by HBoV1 probe clones, created by inserting HBoV1 nt 161-320 (PD1), nt 854–1040 (PA1-2), nt 1998–2160 (PA1-2), nt 1998–2223 (PA1-2/D2), nt 2191–2434 (PA2/D3), nt 2961–3120 (PA3) and nt 3291–3440 [P(pA)p] separately into BamHI/HindIII-digested pGEM4Z vector (Promega). These probes are depicted in Fig. 1A.

(iii) Constructs for glutathione S-transferase (GST)-fusion expression—The HBoV1 NP1 ORF (nt 2410–3067), the C-terminus encoding sequence (nt 2241–2666) of the HBoV1 NS1, and the C-terminus encoding sequence (nt 4160–4480) of the HBoV1 VP1 were cloned into pGEX4T3 (GE Health) as pGEX-HBoVNP1, pGEX-HBoVNS1(aa 640–781) and pGEX-HBoVVP1(aa 369–475), respectively.

All the nucleotide (nt) numbers of HBoV1 and HBoV2 refer to the nucleotide (nt) numbers of the HBoV1 KU2 isolate (Genbank accession no.: GQ925675) and HBoV2 KU1 isolate (Genbank accession no.: GQ200737). The HBoV1 and HBoV2 genomes were sequenced at the MCLab (www.mclab.com), and all the clones with probes or ORFs were sequenced to ensure their fidelities.

RNA isolation, RNase protection assay (RPA) and Northern blot analysis

p5TRHBoV1 was transfected with pHIVAV5Rep and pHelper plasmids as previously described into 293 cells (Guan et al., 2008). pHBoV1 was transfected into 60 to 80% confluency of A549 cells. Total RNA was isolated 48 hrs later by using Trizol reagent (Invitrogen). From this total RNA, mRNA was further purified using the FastTrack MAG Micro mRNA isolation kit (Invitrogen).

Probes were generated, and RPAs were performed as previously described (Naeger et al., 1992; Schoborg and Pintel, 1991; Guan et al., 2008). Northern analyses were performed exactly as previously described (Pintel et al., 1983), using mRNA samples and ^{32}P-labeled DNA probes as indicated.

Antibody production

The antiserum production protocol has been described in our previous publication (Sun et al., 2009). Proteins used for immunizing animals were purified as GST-HBoV1NS1(aa 640–781), GST-HBoV1NP1 and GST-HBoV1VP1/2 (aa 369–475). All animal procedures were approved by the KUMC IACUC.

SDS-PAGE, Western blotting and immunofluorescence

SDS-PAGE, Western blotting and immunofluorescence assay were performed as described previously (Guan et al., 2008; Sun et al., 2009; Qiu et al., 2000). Confocal images were taken at a magnification of $60\times$ (objective lens) with an Eclipse C1 Plus confocal microscope (Nikon) and acquired by Nikon EZ-C1 software.

Flow cytometry analysis

FLICA (Fluorochrome-labeled Inhibitor of Caspase) assay—Cells were dissociated by 0.25% trypsin in Versene and stained with carboxyfluorescein(FAM)-labeled FLICA peptides(Immunochemistry Tech, MN), FAM-VAD-FMK (Poly-FLICA), as described previously (Cheng et al., 2009; Chen et al., 2010).

For co-staining with anti-NS1 of HBoV1, fixed cells were permeabilized in PBS-2%FCS containing 0.2% Tween-20 (PBST) for 30 min, stained with a 1: 50 dilution of anti-NS1 antiserum, followed by staining with a Cy5-labeled secondary antibody.

DAPI staining—Transfected cells were dissociated by 0.25% trypsin in Versene and fixed in 1% paraformaldehyde at RT for 30 min. The cells were washed, stained with DAPI, 4′,6-diamidino-2-phenylindole, at 20 µg/ml in PBST, and then analyzed by flow cytometry. Anti-NS1 costaining was performed as described above.

The samples were analyzed on a three-laser flow cytometer (LSR II, BD Biosciences) within an hour of staining at the Flow Cytometry Core of the University of Kansas Medical Center. Flow cytometry data were analyzed using FACS DIVA software (BD Biosciences).

Acknowledgments

References

Albuquerque MC, Rocha LN, Benati FJ, Soares CC, Maranhao AG, Ramirez ML, Erdman D, Santos N. Human bocavirus infection in children with gastroenteritis, Brazil. Emerg Infect Dis 2007;13:1756–1758. [PubMed: 18217564]

Allander T, Jartti T, Gupta S, Niesters HG, Lehtinen P, Osterback R, Vuorinen T, Waris M, Bjerkner A, Tiveljung-Lindell A, van den Hoogen BG, Hyypia T, Ruuskanen O. Human bocavirus and acute wheezing in children. Clin Infect Dis 2007;44:904–910. [PubMed: 17342639]

Allander T, Tammi MT, Eriksson M, Bjerkner A, Tiveljung-Lindell A, Andersson B. Cloning of a human parvovirus by molecular screening of respiratory tract samples. Proc Natl Acad Sci U S A 2005;102:12891–12896. [PubMed: 16118271]

Arden KE, McErlean P, Nissen MD, Sloots TP, Mackay IM. Frequent detection of human rhinoviruses, paramyxoviruses, coronaviruses, and bocavirus during acute respiratory tract infections. J Med Virol 2006;78:1232–1240. [PubMed: 16847968]

Arnold JC, Singh KK, Spector SA, Sawyer MH. Human bocavirus: prevalence and clinical spectrum at a children's hospital. Clin Infect Dis 2006;43:283–288. [PubMed: 16804840]

Arthur JL, Higgins GD, Davidson GP, Givney RC, Ratcliff RM. A novel bocavirus associated with acute gastroenteritis in Australian children. PLoS Pathog 2009;5:e1000391. [PubMed: 19381259]

Bastien N, Brandt K, Dust K, Ward D, Li Y. Human Bocavirus infection, Canada. Emerg Infect Dis 2006;12:848–850. [PubMed: 16704852]

Best SM, Shelton JF, Pompey JM, Wolfinbarger JB, Bloom ME. Caspase cleavage of the nonstructural protein NS1 mediates replication of Aleutian mink disease parvovirus. J Virol 2003;77:5305–5312. [PubMed: 12692232]

Brandenburger A, Legendre D, Avalosse B, Rommelaere J. NS-1 and NS-2 proteins may act synergistically in the cytopathogenicity of parvovirus MVMp. Virology 1990;174:576–584. [PubMed: 2137660]

Chen AY, Luo Y, Cheng F, Sun Y, Qiu J. Bocavirus infection induces a mitochondrion-mediated apoptosis and cell cycle arrest at G2/M-phase. J Virol. 2010 Mar 24; [Epub ahead of print].

Chen AY, Zhang EY, Guan W, Cheng F, Kleiboeker S, Yankee TM, Qiu J. The small 11kDa non-structural protein of human parvovirus B19 plays a key role in inducing apoptosis during B19 virus infection of primary erythroid progenitor cells. Blood 2010;115:1070–1080. [PubMed: 19861680]

Chen KC, Shull BC, Moses EA, Lederman M, Stout ER, Bates RC. Complete nucleotide sequence and genome organization of bovine parvovirus. J Virol 1986;60:1085–1097. [PubMed: 3783814]

Cheng F, Chen AY, Best SM, Bloom ME, Pintel D, Qiu J. The capsid proteins of Aleutian mink disease virus (AMDV) activate caspases and are specifically cleaved during infection. J Virol 2010;84:2687–2696. [PubMed: 20042496]

Choi EH, Lee HJ, Kim SJ, Eun BW, Kim NH, Lee JA, Lee JH, Song EK, Kim SH, Park JY, Sung JY. The association of newly identified respiratory viruses with lower respiratory tract infections in Korean children, 2000–2005. Clin Infect Dis 2006;43:585–592. [PubMed: 16886150]

Choi EY, Newman AE, Burger L, Pintel D. Replication of minute virus of mice DNA is critically dependent on accumulated levels of NS2. J Virol 2005;79:12375–12381. [PubMed: 16160164]

Cotmore, SF.; Tattersall, P. Structure and Organization of the Viral Genome. In: Kerr, J.; Cotmore, SF.; Bloom, ME.; Linden, RM.; Parrish, CR., editors. Parvoviruses. London: Hodder Arnold; 2005. p. 73-94.

Cotmore, SF.; Tattersall, P. A rolling-haipin strategy: basic mechanisms of DNA replication in the parvoviruses. In: Kerr, J.; Cotmore, SF.; Bloom, ME.; Linden, RM.; Parrish, CR., editors. Parvoviruses. London: Hoddler Arond; 2006. p. 171-181.

Daeffler L, Horlein R, Rommelaere J, Nuesch JP. Modulation of minute virus of mice cytotoxic activities through site-directed mutagenesis within the NS coding region. J Virol 2003;77:12466–12478. [PubMed: 14610171]

Degterev A, Boyce M, Yuan J. A decade of caspases. Oncogene 2003;22:8543–8567. [PubMed: 14634618]

Dijkman R, Koekkoek SM, Molenkamp R, Schildgen O, van der Hoek L. Human bocavirus can be cultured in differentiated human airway epithelial cells. J Virol 2009;83:7739–7748. [PubMed: 19474096]

Foulongne V, Olejnik Y, Perez V, Elaerts S, Rodiere M, Segondy M. Human bocavirus in French children. Emerg Infect Dis 2006;12:1251–1253. [PubMed: 16965707]

Guan W, Cheng F, Yoto Y, Kleiboeker S, Wong S, Zhi N, Pintel DJ, Qiu J. Block to the production of full-length B19 virus transcripts by internal polyadenylation is overcome by replication of the viral genome. J Virol 2008;82:9951–9963. [PubMed: 18684834]

Kahn J. Human bocavirus: clinical significance and implications. Curr Opin Pediatr 2008;20:62–66. [PubMed: 18197041]

Kantola K, Hedman L, Allander T, Jartti T, Lehtinen P, Ruuskanen O, Hedman K, Soderlund-Venermo M. Serodiagnosis of human bocavirus infection. Clin Infect Dis 2008;46:540–546. [PubMed: 18199037]

Kapoor A, Slikas E, Simmonds P, Chieochansin T, Naeem A, Shaukat S, Alam MM, Sharif S, Angez M, Zaidi S, Delwart E. A Newly Identified Bocavirus Species in Human Stool. J Infect Dis 2009;199:196–200. [PubMed: 19072716]

Larkin MA, Blackshields G, Brown NP, Chenna R, McGettigan PA, McWilliam H, Valentin F, Wallace IM, Wilm A, Lopez R, Thompson JD, Gibson TJ, Higgins DG. Clustal W and Clustal X version 2.0. Bioinformatics 2007;23:2947–2948. [PubMed: 17846036]

Lau SK, Yip CC, Que TL, Lee RA, Au-Yeung RK, Zhou B, So LY, Lau YL, Chan KH, Woo PC, Yuen KY. Clinical and molecular epidemiology of human bocavirus in respiratory and fecal samples from children in Hong Kong. J Infect Dis 2007;196:986–993. [PubMed: 17763318]

Lederman M, Bates RC, Stout ER. In vitro and in vivo studies of bovine parvovirus proteins. J Virol 1983;48:10–17. [PubMed: 6887348]

Lederman M, Cotmore SF, Stout ER, Bates RC. Detection of bovine parvovirus proteins homologous to the nonstructural NS-1 proteins of other autonomous parvoviruses. J Virol 1987;61:3612–3616. [PubMed: 2959794]

Lee JI, Chung JY, Han TH, Song MO, Hwang ES. Detection of human bocavirus in children hospitalized because of acute gastroenteritis. J Infect Dis 2007;196:994–997. [PubMed: 17763319]

Lin F, Guan W, Cheng F, Yang N, Pintel D, Qiu J. ELISAs using human bocavirus VP2 virus-like particles for detection of antibodies against HBoV. J Virol Methods 2008;149:110–117. [PubMed: 18289709]

Lin F, Zeng A, Yang N, Lin H, Yang E, Wang S, Pintel D, Qiu J. Quantification of human bocavirus in lower respiratory tract infections in China. Infect Agent Cancer 2007;2:3. [PubMed: 17266760]

Liu Z, Qiu J, Cheng F, Chu Y, Yoto Y, O'Sullivan MG, Brown KE, Pintel DJ. Comparison of the transcription profile of simian parvovirus with that of the human erythrovirus B19 reveals a number of unique features. J Virol 2004;78:12929–12939. [PubMed: 15542645]

Ma X, Endo R, Ishiguro N, Ebihara T, Ishiko H, Ariga T, Kikuta H. Detection of human bocavirus in Japanese children with lower respiratory tract infections. J Clin Microbiol 2006;44:1132–1134. [PubMed: 16517912]

Naeger LK, Schoborg RV, Zhao Q, Tullis GE, Pintel DJ. Nonsense mutations inhibit splicing of MVM RNA in cis when they interrupt the reading frame of either exon of the final spliced product. Genes Dev 1992;6:1107–1119. [PubMed: 1592259]

Nuesch JP, Rommelaere J. NS1 interaction with CKII alpha: novel protein complex mediating parvovirus-induced cytotoxicity. J Virol 2006;80:4729–4739. [PubMed: 16641266]

Ozawa K, Ayub J, Hao YS, Kurtzman G, Shimada T, Young N. Novel transcription map for the B19 (human) pathogenic parvovirus. J Virol 1987;61:2395–2406. [PubMed: 3599180]

Ozawa K, Ayub J, Kajigaya S, Shimada T, Young N. The gene encoding the nonstructural protein of B19 (human) parvovirus may be lethal in transfected cells. J Virol 1988;62:2884–2889. [PubMed: 2969055]

Pintel D, Dadachanji D, Astell CR, Ward DC. The genome of minute virus of mice, an autonomous parvovirus, encodes two overlapping transcription units. Nucleic Acids Res 1983;11:1019–1038. [PubMed: 6828378]

Qiu J, Cheng F, Burger LR, Pintel D. The transcription profile of Aleutian Mink Disease Virus (AMDV) in CRFK cells is generated by alternative processing of pre-mRNAs produced from a single promoter. J Virol 2006;80:654–662. [PubMed: 16378968]

Qiu J, Cheng F, Johnson FB, Pintel D. The transcription profile of the bocavirus bovine parvovirus is unlike those of previously characterized parvoviruses. J Virol 2007;81:12080–12085. [PubMed: 17715221]

Qiu J, Cheng F, Yoto Y, Zadori Z, Pintel D. The expression strategy of goose parvovirus exhibits features of both the Dependovirus and Parvovirus genera. J Virol 2005;79:11035–11044. [PubMed: 16103154]

Qiu J, Handa A, Kirby M, Brown KE. The interaction of heparin sulfate and adeno-associated virus 2. Virology 2000;269:137–147. [PubMed: 10725206]

Qiu J, Nayak R, Tullis GE, Pintel DJ. Characterization of the transcription profile of adeno-associated virus type 5 reveals a number of unique features compared to previously characterized adeno-associated viruses. J Virol 2002;76:12435–12447. [PubMed: 12438569]

Qiu J, Pintel D. Processing of adeno-associated virus RNA. Front Biosci 2008;13:3101–3115. [PubMed: 17981780]

Qiu J, Pintel DJ. The adeno-associated virus type 2 Rep protein regulates RNA processing via interaction with the transcription template. Mol Cell Biol 2002;22:3639–3652. [PubMed: 11997501]

Rayet B, Lopez-Guerrero JA, Rommelaere J, Dinsart C. Induction of programmed cell death by parvovirus H-1 in U937 cells: connection with the tumor necrosis factor alpha signalling pathway. J Virol 1998;72:8893–8903. [PubMed: 9765434]

Schildgen O, Muller A, Allander T, Mackay IM, Volz S, Kupfer B, Simon A. Human bocavirus: passenger or pathogen in acute respiratory tract infections? Clin Microbiol Rev 2008;21:291–304. [PubMed: 18400798]

Schmidt M, Afione S, Kotin RM. Adeno-associated virus type 2 Rep78 induces apoptosis through caspase activation independently of p53. J Virol 2000;74:9441–9450. [PubMed: 11000213]

Schoborg RV, Pintel DJ. Accumulation of MVM gene products is differentially regulated by transcription initiation, RNA processing and protein stability. Virology 1991;181:22–34. [PubMed: 1825251]

Schwartz D, Green B, Carmichael LE, Parrish CR. The canine minute virus (minute virus of canines) is a distinct parvovirus that is most similar to bovine parvovirus. Virology 2002;302:219–223. [PubMed: 12441065]

Sloots TP, McErlean P, Speicher DJ, Arden KE, Nissen MD, Mackay IM. Evidence of human coronavirus HKU1 and human bocavirus in Australian children. J Clin Virol 2006;35:99–102. [PubMed: 16257260]

Sol N, Le JJ, Vassias I, Freyssinier JM, Thomas A, Prigent AF, Rudkin BB, Fichelson S, Morinet F. Possible interactions between the NS-1 protein and tumor necrosis factor alpha pathways in erythroid cell apoptosis induced by human parvovirus B19. J Virol 1999;73:8762–8770. [PubMed: 10482630]

Sun Y, Chen AY, Cheng F, Guan W, Johnson FB, Qiu J. Molecular characterization of infectious clones of the minute virus of canines reveals unique features of bocaviruses. J Virol 2009;83:3956–3967. [PubMed: 19211770]

Vicente D, Cilla G, Montes M, Perez-Yarza EG, Perez-Trallero E. Human bocavirus, a respiratory and enteric virus. Emerg Infect Dis 2007;13:636–637. [PubMed: 17553287]

Vihinen-Ranta, M.; Parish, CR. Cell infection process of autonomous parvovirus. In: Kerr, JR.; Cotmore, SF.; Bloom, ME.; Linden, ME.; Parrish, CR., editors. Parvoviruses. London: Hodder Arnold; 2006. p. 157-163.

Weissbrich B, Neske F, Schubert J, Tollmann F, Blath K, Blessing K, Kreth HW. Frequent detection of bocavirus DNA in German children with respiratory tract infections. BMC Infect Dis 2006;6:109, 109. [PubMed: 16834781]

Young NS, Brown KE. Mechanism of disease:Parvovirus B19. N Engl J Med 2004;350:586–597. [PubMed: 14762186]
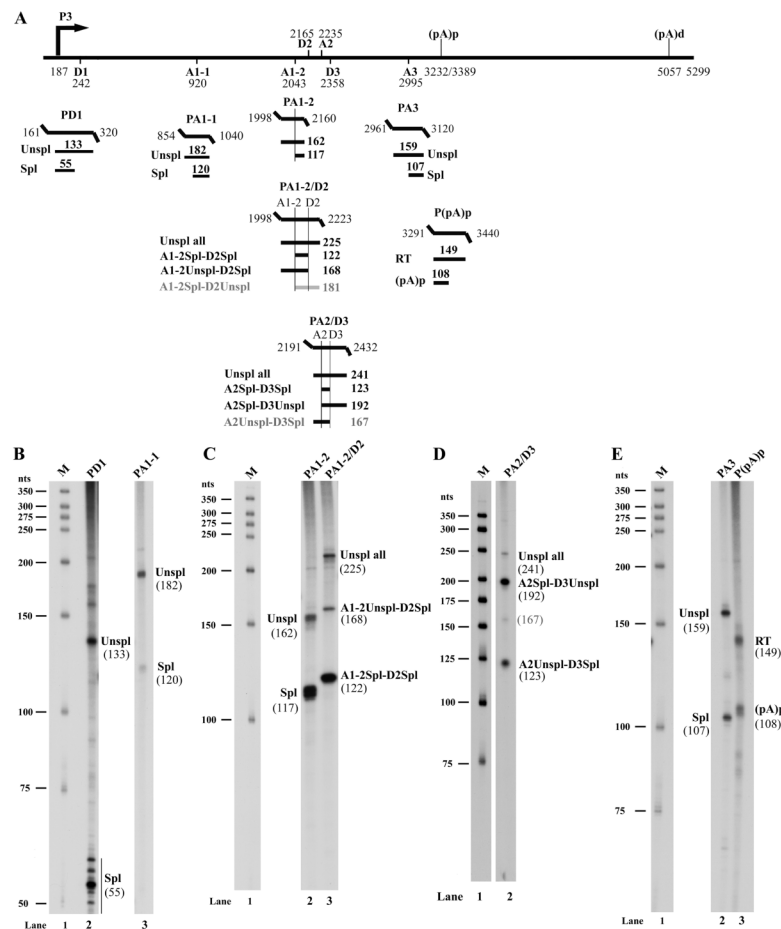
Figure 1. Transcription mapping of HBoV1 RNA by RPA

(A) Schematic diagram of the HBoV1 genome and the probes used for RPA. The landmarks of transcription: the promoter (P3), the splice donor sites (D1, D2, and D3), the acceptor sites (A1-1, A1-2, A2 and A3), the internal polyadenylation signal (pA)p and the distal polyadenylation site (pA)d, which were identified by RT-PCR and RACE, are shown. The RPA probes PD1 (nt 161 to 320), PA1-1 (nt 854 to 1040), PA1-2 (nt 1998–2160), PA1-2/D2 (1998–2223), PA2/D3 (nt 2191–2432), PA3 (nt 2961–3120) and p(pA)p (nt 3291–3440) are shown, along with the designated bands they are expected to protect and their predicted sizes.

(B, C, D&E) Mapping of the HBoV1 transcription map by RPA. Ten μg of total RNA isolated 2 days from p5TRHBoV1-transfected 293 cells was protected by the above described probes, in individual reactions as indicated. Lane 1, ^{32}P-labeled RNA markers (Qiu et al., 2002), with sizes indicated to the left. The origins of the protected bands in the lanes are indicated. Spl, spliced RNAs; Unspl, unspliced RNAs; RT, RNAs read through the (pA)p site; (pA)p, polyadenylated RNAs at (pA)p.
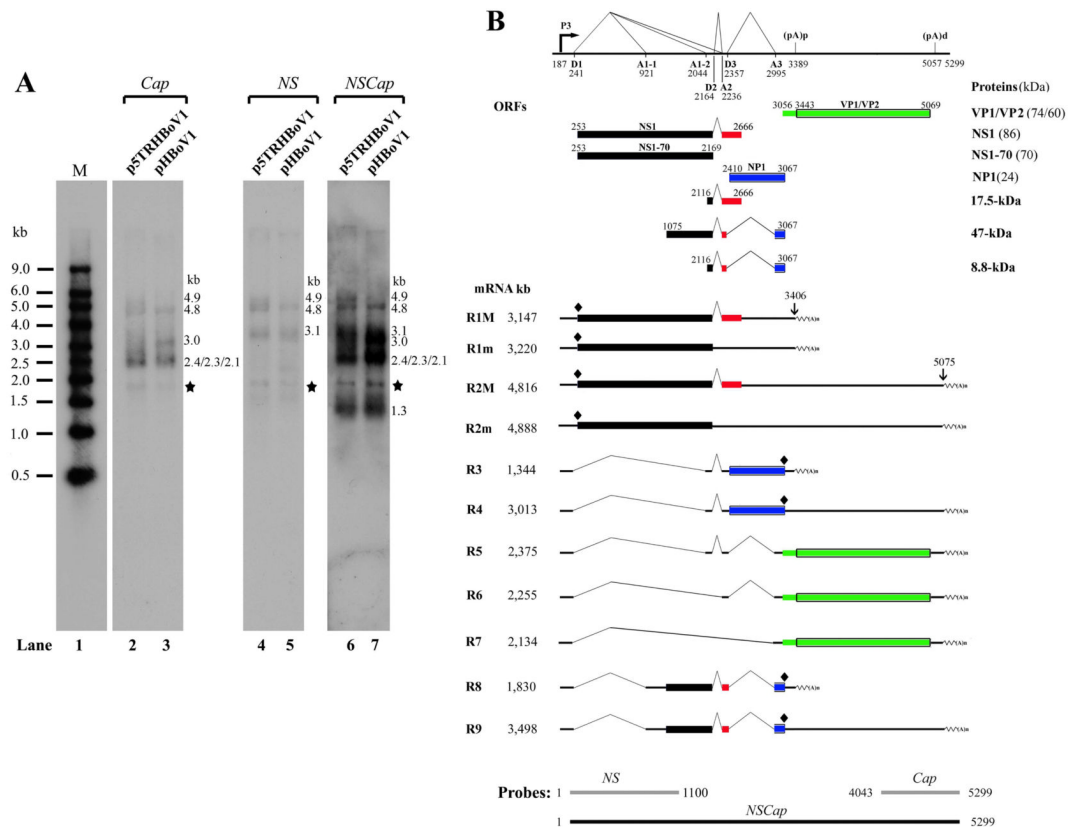
Figure 2. Transcription profile of HBoV1 RNA
(A) Northern blot analysis of HBoV1 RNA. Total RNAs were extracted from p5TRHBoV1-transfected 293 cells or pHBoV1-transfected A549 cells, mRNAs purified from 5 μg or 20 μg of the total RNAs were loaded in the lane as indicated for Northern blot. The blots were hybridized to *NS*, *Cap* and *NSCap* probes, respectively, which are diagramed at the bottom of panel B with their specific locations. The size of each detected bands is shown to the right of each lane. The identities of each band are illustrated in panel B. RNA maker ladder (Ambion) is shown in lane 1. The asterisk indicates a band at approximately 1.8 kb, which was detected by all the three probes. **(B) Putative transcription map of HBoV1.** The genome of HBoV1 is shown to scale with transcription landmarks, including the P3 promoter, splice donor (D1, D2 and D3) and acceptor (A1-1, A1-2, A2 and A3) sites, the internal polyadenylation site [(pA) p], and the distal polyadenylation site [(pA)d]. All of the RNA species are proposed from results of RT-PCR and RPA and shown with their respective sizes (minus a poly A tail of approximately 150 nts). The putative ORFs are diagramed with their predicated size in kDa of translated proteins. The cleavage sites are shown by arrows with respective nucleotide numbers. HA-tagged ORFs are indicated by a "diamond" symbol.
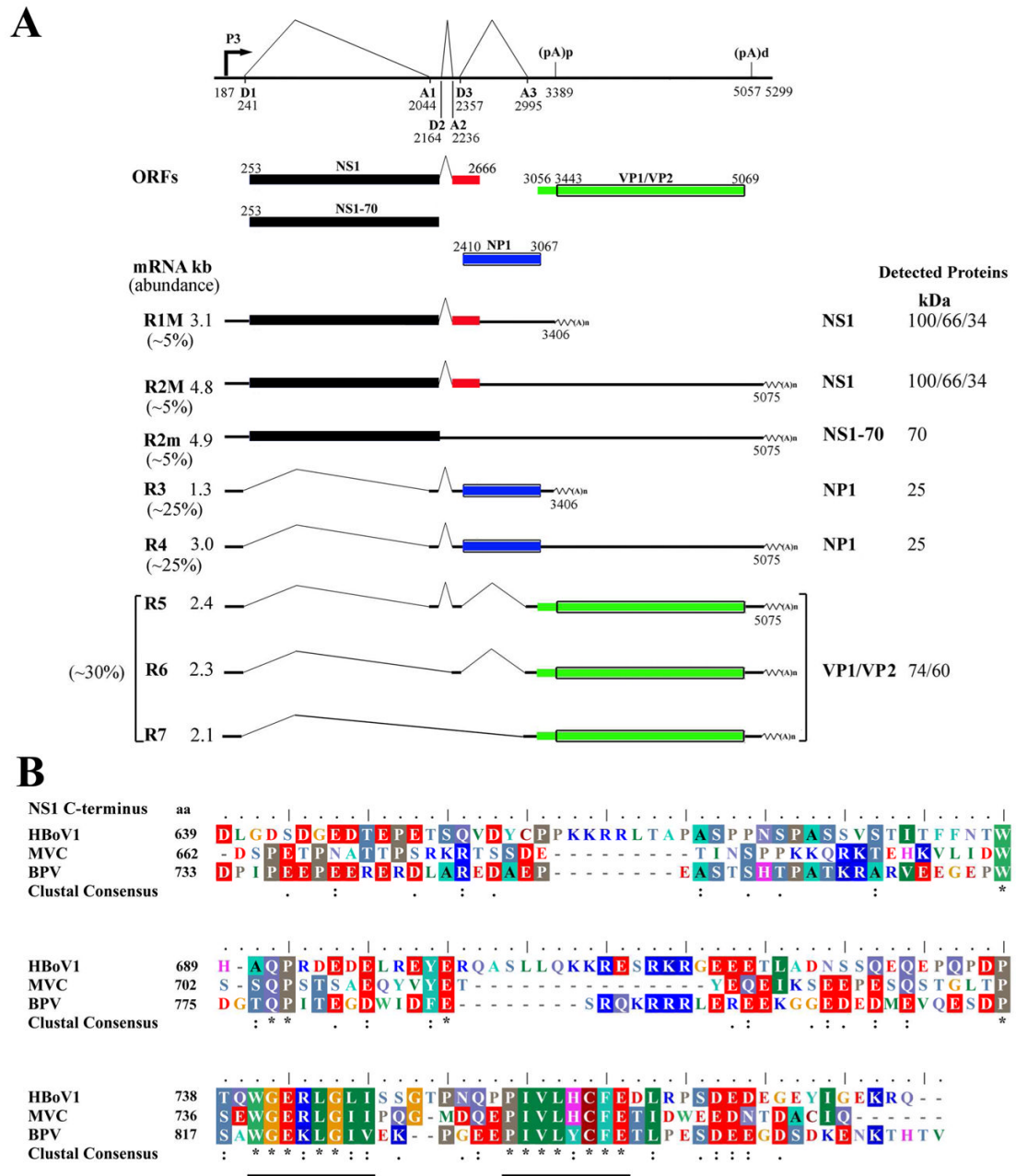
Figure 3. Genetic map of HBoV1 and alignment of *Bocavirus* NS1 C-terminus
(A) A summarized genetic map of HBoV1 is shown with transcription landmarks in panel A. Six major species of HBoV1 transcripts that were confirmed by Northern blot analysis are shown with their relative abundance and sizes (minus a poly A tail of approximately 150 nts). Proteins detected by transfection are indicated. (B) Comparison of the NS1 C-termini of HBoV1, BPV and MVC. The C-terminus aa 639–781 of HBoV NS1, aa 662–774 of MVC NS1, and aa 733–860 BPV NS1 were chosen to align using ClustalW2 (Larkin et al., 2007). Identical amino acids are shown as a "star" symbol, while homology amino acids shown as two dots under the amino acid sequences of the C-termini. Conserved motifs are underlined.
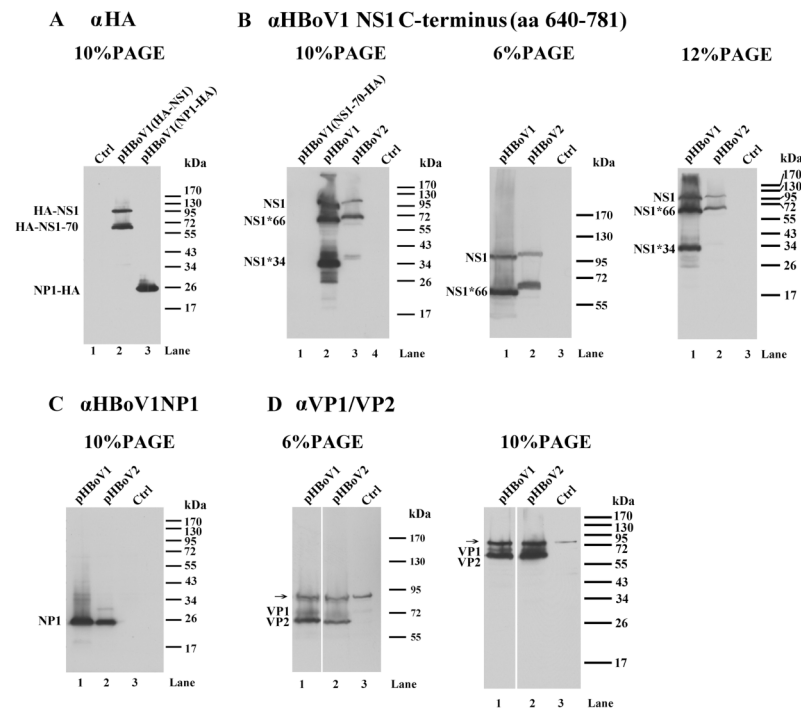
Figure 4. Expression of HBoV proteins
(A) Western blot analysis of HBoV1 protein by transfection of HA-tagged constructs.
A549 cells were transfected with HA-tagged constructs as indicated. Two days
posttransfection, cells were lysed for Western blot using a monoclonal antibody against HA
tag (HA-7, Sigma). **(B, C&D) Western blot analysis of HBoV1 and HBoV2 proteins by
transfection.** A549 cells were transfected with the nearly full-length clones of pHBoV1 and
pHBoV2 as indicated. Two days later, cells were lysed for Western blot using anti-HBoV1NS1
**(B)**, anti-HBoV1NP1 **(C)**, and anti-HBoV1VP1/2, respectively.
The identities of detected proteins are shown to the left on the blot. Small bands of the NS1 at
66 and 34 kDa that retain the C-terminus are shown as NS1*66 and NS1*34, respectively.
pBluescript SK(+)-transfected cells were used as control (Ctrl).
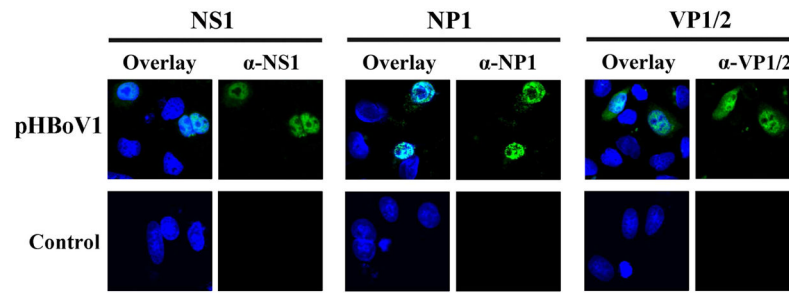
Figure 5. Cellular localization of HBoV1 proteins by transfection
A549 cells were transfected with the pHBoV1 construct. At 48 hrs posttransfection, cells were stained with anti-NS1, anti-NP1 and anti-VP1/2, respectively. Confocal images were taken at × 60 magnification (objective lens). Nuclei were stained with DAPI. pBluescript SK(+)-transfected cells were used as control (Control).
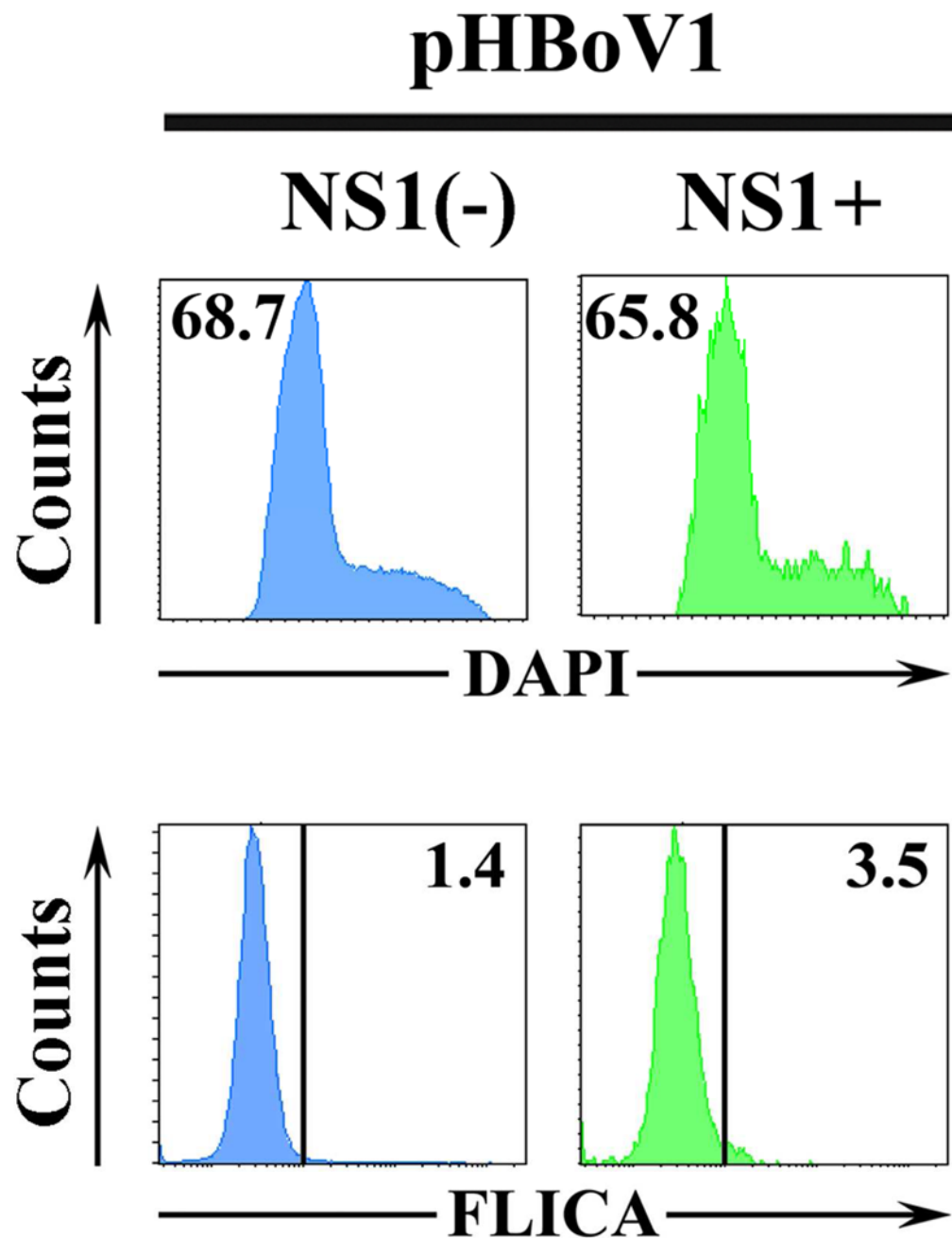
Figure 6. Expressing of HBoV1 proteins does not induce cell cycle arrest or activate caspases
A549 cells were transfected with the pHBoV1. The transfected cells were stained with DAPI and anti-NS1 for cell cycle analysis and pan-FLICA and anti-NS1 for detection of apoptosis, respectively, at 48 hrs posttransfection. Numbers shown in DAPI staining are percentage of cells at the G0/G1 phase, and numbers shown in FLICA staining are percentage of pan-FLICA positive cells. A representative result is shown from two independent experiments.